ELSEVIER

Coordination Chemistry Reviews 226 (2002) 167–178

COORDINATION CHEMISTRY REVIEWS

www.elsevier.com/locate/ccr

Synthesis and reactivity of (phosphinoaklyl)silyl complexes

Masaaki Okazaki *, Shin Ohshitanai, Masatoshi Iwata, Hiromi Tobita, Hiroshi Ogino

Department of Chemistry, Graduate School of Science, Tohoku University, Sendai 980-8578, Japan

Received 23 May 2001; accepted 17 August 2001

Contents

Abstract

Silyl ancillary ligands are expected to generate the reactive unsaturated metal center due to their exceptionally strong *trans*-influence and -effect. Nevertheless, little has been known on the influence of silyl ligands on the reactivity of transition-metal complexes. This would be mainly due to the facile cleavage of the metal–silicon bond. (Phosphinoalkyl)silyl ligands have been developed to suppress the elimination of silyl groups from the metal center. This article reviews the synthesis and properties of the transition metal complexes having chelate-type (phosphinoalkyl)silyl ligands $R_2P(CH_2)_nSiR_2$ ($n = 1, 2$). © 2002 Elsevier Science B.V. All rights reserved.

Keywords: (Phosphinoalkyl)silyl; (Phosphinoethyl)silyl; (Phosphinomethyl)silyl; Chelate; Silyl complex; Ancillary ligand

1. Introduction

Complexation of a silicon atom to a metal center has a great impact on the various parameters of the complex which provide good evidence for the exceptionally strong σ-donor character and high *trans*-influencing ability of the ligated silicon [1]. Taking into account its character, silyl groups are expected to be an excellent ancillary ligand generating an electron-rich metal center. Milstein et al. reported the C–F bond activation of polyfluorobenzene by a silylrhodium(I) complex $(Me_3P)_3RhSiMe_2Ph$ [2]. However, little has been investigated on the influence of silyl ligands on the reactivity of transition-metal complexes. This would be mainly due to the facile cleavage of metal–silicon bonds via reductive elimination, nucleophilic attack at the silyl silicon atom, insertion, and σ-bond metathesis [3]. (Phosphinoalkyl)silyl ligands have been developed to suppress the elimination of the silyl groups from the metal center. They are usually bound to the metal center via coordination of silicon and phosphorus atoms. Extrusion of the silyl groups from the metal center is greatly retarded by the chelate effect. This article reviews the synthesis and properties of the tran-

---

* Corresponding author. Tel.: +81-22-217-6541; fax: +81-22-217-6543.

E-mail address: ogino@agnus.chem.tohoku.ac.jp (H. Ogino).

PII: S0010-8545(01)00422-2

sition-metal complexes having chelate-type (phosphinoalkyl)silyl ligands $R_2P(CH_2)_nSiR_2$ ($n = 1, 2$).

2. Synthesis of (phosphinoalkyl)silanes

Complexes with η^2-$R_2P(CH_2)_nSiR_2$ have been synthesized by the reaction of coordinatively unsaturated metal complexes with $R_2P(CH_2)_nSiR_2H$ via coordination of the phosphine moiety and the oxidative addition of the Si–H bond (Eq. (1)). Thus, a wide variety of (phosphinoalkyl)silanes with the Si–H bond have been synthesized as the ligand precursor.

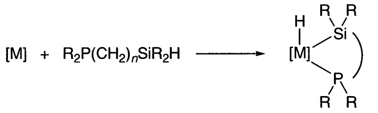

(1)

2.1. $Ph_2PCH_2CH_2SiR_2H$

Compounds with the P–C–C–Si linkage are obtained upon photolysis of the mixture of R_2PH and $(CH_2{=}CH)SiR_3$ in which the anti-Markovnikov radical addition of P–H across an unsaturated vinyl group takes place (Eq. (2)) [4]. (Phosphinoethyl)silanes with SiH were also synthesized by a similar photolysis (Eq. (3)). Addition of Si–H across a vinyl double bond has not been observed in this reaction [5].

$$R_2PH + CH_2 = CHSiR_3 \xrightarrow{hv} R_2PCH_2CH_2SiR_3 \qquad (2)$$

$$Ph_2PH + CH_2 = CHSiR_2H \xrightarrow{hv} Ph_2PCH_2CH_2SiR_2H$$

$$R = Me, Ph \qquad (3)$$

2.2. $Ph_2PCH_2SiR_2H$

Compounds with the P–C–Si linkage have been synthesized by the reaction of chlorosilanes with R_2PCH_2Li [6]. Treatment of R_2SiCl_2 ($R = Me, Ph$) with 1 equiv. $Ph_2PCH_2Li \cdot tmeda$ and subsequent reduction with $LiAlH_4$ afforded $Ph_2PCH_2SiR_2H$ (Eq. (4)) [4]. $Ph_2PCH_2SiMe_2H$ can also be synthesized by the direct reaction of $HSiMe_2Cl$ with $Ph_2PCH_2Li \cdot tmeda$ [7].

$$\begin{tikzcd}
R_2SiCl_2 + Ph_2PCH_2Li{\cdot}tmeda \arrow[r] & Ph_2PCH_2SiR_2Cl \arrow[d, "+\,LiAlH_4"] \\
tmeda = Me_2NCH_2CH_2NMe_2 & Ph_2PCH_2SiR_2H
\end{tikzcd} \qquad (4)$$

3. Synthesis of η^2-(phosphinoethyl)silyl complexes

3.1. Pd and Pt complexes

The platinum(0) complex $Pt(COD)_2$ reacts with $Ph_2PCH_2CH_2SiHR^1R^2$ to give platinum(II) complexes *cis*-$Pt(\eta^2\text{-}R^1R^2SiCH_2CH_2PPh_2)_2$ (Eq. (5)) [8]. According to X-ray crystal structure analysis, complex **1** has a typical square-planar platinum(II) environment in which two phosphorus atoms occupy the mutually *cis* position. Taking account of the strong *trans*-influence of the silyl ligands, the *cis* geometry is quite reasonable. Addition of $Ph_2PCH_2CH_2SiMe_2H$ to platinum(II) complexes $PtX(Cl)(COD)$ ($X = Cl, Me$) in the presence of NEt_3 also leads to the formation of **1** (Eq. (6)).

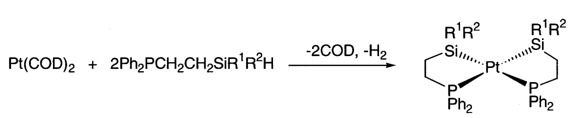

1; $R^1 = R^2 = Me$
2; $R^1 = R^2 = Ph$
3; $R^1 = Me, R^2 = Ph$
4; $R^1 = H, R^2 = Me$
5; $R^1 = H, R^2 = Ph$

(5)

$$\underset{X = Cl, Me}{PtX(Cl)(COD)} + 2Ph_2PCH_2CH_2SiMe_2H \xrightarrow[\substack{-HNEt_3Cl \\ -COD}]{+NEt_3} \mathbf{1} \qquad (6)$$

Treatment of $PtMe_2(COD)$ with 2 equiv. $Ph_2PCH_2CH_2SiMe_2H$ forms the platinum(II) complex $Pt(\eta^2\text{-}Me_2SiCH_2CH_2PPh_2)_2$ (**1**) via elimination of methane (Eq. (7)) [9].

$$PtMe_2(COD) + Ph_2PCH_2CH_2SiMe_2H \xrightarrow[-2MeH]{} \mathbf{1} \qquad (7)$$

The synthesis of η^2-(phosphinoethyl)silyl complexes through the oxidative addition of Si–E (E = C, Sn) has also been reported. The reaction of a palladium(0) complex with $Ph_2PCH_2CH_2SiMe_2SnMe_3$ gives the bis{η^2-(2-phosphinoethyl)silyl}palladium(II) complex **6** via oxidative addition of the Si–Sn bond (Eq. (8)) [10]. Heating $Pt(C_2H_4)(PPh_3)_2$ with $Ph_2PCH_2CH_2SiR_2Ph$ ($R_2 = Ph_2$, PhMe) at 70 °C affords the platinum(II) complexes **7** and **8** via Si–Ph oxidative addition (Eq. (9)). The Si–Me oxidative addition product has not been confirmed [11].

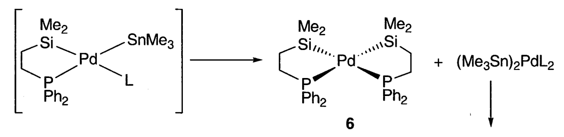

6

L = two-electron donor

(8)

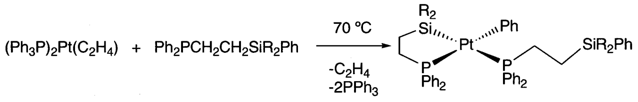

7; $R_2 = Ph_2$
8; $R_2 = PhMe$

(9)

3.2. Rh and Ir complexes

When reaction of a coordinatively unsaturated iridium(I) complex $IrCl(CO)(PPh_3)_2$ (Vaska's complex) with (phosphinoethyl)silanes $Ph_2PCH_2CH_2SiR^1R^2H$ is performed, the six-coordinate octahedral iridium(III) complexes are formed (Eq. (10)) [12]. The spectroscopic data established the geometry of the iridium(III) complexes **9**–**13**. The strongly *trans*-influencing silyl ligand is reasonably located at the position opposite to the least *trans*-influencing chloro ligand.

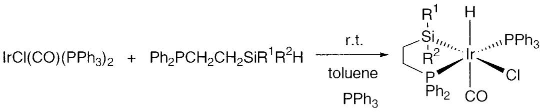

(10)

9; $R^1 = R^2 =$ Me
10; $R^1 = R^2 =$ Ph
11; $R^1 =$ Me, $R^2 =$ Ph
12; $R^1 =$ Me, $R^2 =$ H
13; $R^1 =$ Ph, $R^2 =$ H

Treatment of $IrCl(H)(\eta^2\text{-}Me_2SiCH_2CH_2PPh_2)(CO)(PPh_3)$ (**9**) with $LiAlH_4$ in THF forms $IrH_2(\eta^2\text{-}Me_2SiCH_2CH_2PPh_2)(CO)(PPh_3)$ (**14**) (Eq. (11)) [12]. Formation of **14** is accompanied by the rearrangement of ligands. The silyl ligand of **14** is located at the *trans*-position of the phosphine ligand rather than the strongly *trans*-influencing CO or hydrido ligands. This complex is independently synthesized by the reaction of $IrH(CO)(PPh_3)_3$ with $Ph_2PCH_2CH_2SiMe_2H$ at room temperature (r.t.) (Eq. (12)) [12].

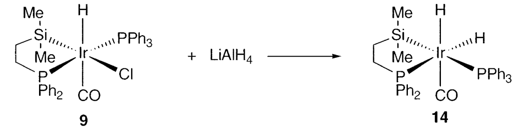

(11)

$$IrH(CO)(PPh)_3 + Ph_2PCH_2CH_2SiMe_2H \xrightarrow{-2PPh_3} \mathbf{14} \quad (12)$$

Complex **9** reacts with $Ph_2PCH_2CH_2SiMe_2H$ in the presence of NEt_3 to give $IrH(\eta^2\text{-}Me_2SiCH_2CH_2PPh_2)_2(CO)$ (**15**) in which two (phosphinoethyl)silyl chelate ligands are chemically equivalent (Eq. (13)) [12]. Complex **15** is also synthesized by the reaction of $IrH_2(\eta^2\text{-}Me_2SiCH_2CH_2PPh_2)(CO)(PPh_3)$ (**14**) with $Ph_2PCH_2CH_2SiMe_2H$ via evolution of H_2 (Eq. (13)) [12].

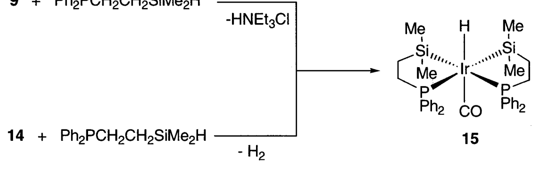

(13)

Reaction of $[Ir(COD)Cl]_2$ with $Ph_2PCH_2CH_2SiMe_2H$ proceeds step by step at r.t. $[Ir(COD)Cl]_2$ reacts with 2 equiv. $Ph_2PCH_2CH_2SiMe_2H$ to give $IrH(Cl)(\eta^2\text{-}Me_2SiCH_2CH_2PPh_2)(COD)$ (**16**) (Eq. (14)). In the reaction with 4 equiv. $Ph_2PCH_2CH_2SiMe_2H$, $IrCl(\eta^2\text{-}Me_2SiCH_2CH_2PPh_2)_2$ (**17**) is formed via evolution of H_2. The rhodium dimer $[Rh(COD)Cl]_2$ reacts with $Ph_2PCH_2CH_2SiMe_2H$ to give $RhCl(\eta^2\text{-}Me_2SiCH_2CH_2PPh_2)_2$ (**18**) exclusively, and the rhodium analog of **16** was not detected under the same reaction conditions as those of Eq. (14) [13].

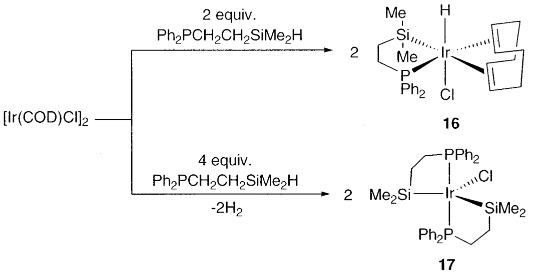

(14)

The bis{η^2-(phosphinoethyl)silyl}iridium(III) complex **18** is obtained by the reaction of Vaska's complex with $Ph_2PCH_2CH_2SiMe_2SiMe_2CH_2CH_2PPh_2$ via oxidative addition of the silicon–silicon bond (Eq. (15)) [14].

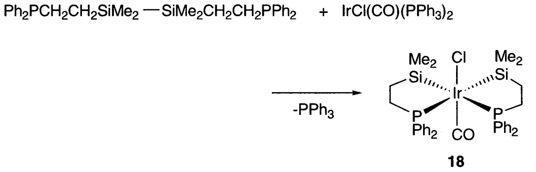

(15)

UV irradiation of the dihydrido complex $IrH_2(\eta^2\text{-}Me_2SiCH_2CH_2PPh_2)(CO)(PPh_3)$ (**14**) in THF (250 h, 450 W medium-pressure Hg lamp) leads to extensive decomposition in which the formation of the iridium(I) complex $Ir(\eta^2\text{-}Me_2SiCH_2CH_2PPh_2)(CO)_2(PPh_3)$ (**20**) was spectroscopically confirmed in low yield (Eq. (16)) [15]. Photolysis of **14** under CO atmosphere was also examined. The photoreaction proceeds almost quantitatively to give **20**. The structure of **20** has been unequivocally determined by X-ray crystal structure analysis to be a five-coordinate trigonal-bipyramidal structure in which silyl and PPh_3 ligands are located at the axial positions. The formation mechanism of **20** may involve the reductive elimination of H_2 accelerated by photolysis to give an extremely reactive silyliridium(I) intermediate **19**. There has been no example for the isolation of such a coordinatively unsaturated silyliridium(I) complex. Intermediate **19** absorbs one carbon monoxide to give **20** [15].

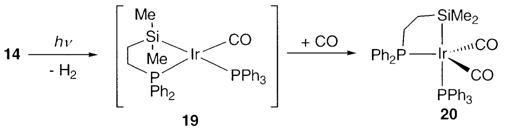

(16)

To synthesize a reactive silylrhodium(I) complex, a tetradentate silyl ligand $\eta^4\text{-}Si(CH_2CH_2PPh_2)_3$ ('tripsi') has been developed. $[Rh(COD)Cl]_2$ reacts with Htripsi to afford the rhodium(III) complex Rh(tripsi)(H)(Cl) (**21**) (Eq. (17)). Treatment of **21** with MeLi under a CO atmosphere leads to the evolution of methane to give a coordinatively saturated silylrhodium(I) complex Rh(tripsi)(CO) (**22**) (Eq. (18)). The reaction may proceed through formation of a Rh(tripsi)(H)(Me) intermediate that undergoes the elimination of methane and coordination of carbon monoxide. According to the X-ray crystal structure analysis, complex **22** adopts a five-coordinate trigonal-bipyramidal structure. Tripsi acts as a tetradentate ligand in which three phosphorus atoms are located on the equatorial plane [16].

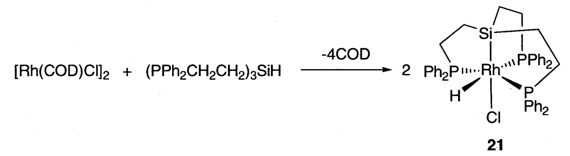

(17)

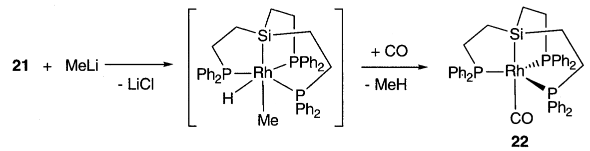

(18)

Our research has been focused on the reactivity of rhodium and iridium complexes having the (2-phosphinoethyl)silyl ligand as an ancillary ligand. In order to obtain an electron-rich metal center suitable for the activation of small molecules, the strongly electron-donating PMe_3 ligands have been employed.

A rhodium(III) complex $RhH(Cl)[\eta^2\text{-}Me_2Si(CH_2)_2\text{-}PPh_2](PMe_3)_2$ (**23**) can be synthesized by the reaction of the Wilkinson-type rhodium(I) complex $RhCl(PMe_3)_3$ with $Ph_2PCH_2CH_2SiMe_2H$ (Eq. (19)) [17]. It is well known that the oxidative addition of hydrosilane to the rhodium(I) complex is reversible. However, the chelate-assisted oxidative addition in Eq. (19) takes place irreversibly. The ORTEP drawing of **23** is illustrated in Fig. 1. Complex **23** adopts a six-coordinate, slightly distorted octahedral arrangement in which three phosphorus atoms takes a meridional position. The Si–Rh–P1 bite angle of the (2-phosphinoethyl)silyl ligand is 85.10(4)°. Like other silyl complexes, the strongly *trans*-influencing silyl group is located at the *trans* position of the weakly *trans*-influencing chloro group.

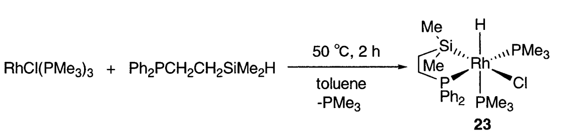

(19)

A coordinatively unsaturated silylrhodium(I) complex $Rh(\eta^2\text{-}Me_2SiCH_2CH_2PPh_2)(PMe_3)_2$ (**24**) can be prepared from the reaction of **23** with 1 equiv. MeLi (Eq. (20)) [17]. The reaction may proceed via formation of the hydrido(methyl)rhodium(III) intermediate $Rh(H)(Me)\{\eta^2\text{-}Me_2SiCH_2CH_2PPh_2\}(PMe_3)_2$ (**25**), although the intermediate **25** was not detected by NMR spectroscopy in the course of the reaction. Complex **24** is extremely air-sensitive compared with $RhCl(PMe_3)_3$, indicating that the presence of the electron releasing silyl group makes **24** electron rich. The ORTEP drawing indicates that **24** is among the few coordinatively unsaturated silylrhodium(I) complexes and adopts a slightly distorted square-planar geometry (Fig. 2). The angles P1–Rh–P2 and P3–Rh–Si are 167.65(3) and 176.58(2) Å, respectively. The Rh–Si bond length is 2.3937(8) Å and relatively longer than those of the previously reported silylrhodium(I) complexes $(Ph_3Si)Rh(PMe_3)_3$ [2.317(1) Å] [18] and $(PhMe_2Si)Rh(PMe_3)_3$ [2.3804(10) Å] [2]. The difference in the Rh–Si bond distances is attributable to the degree of the M(dπ)–SiX(σ*) interaction [19]. The efficiency of the interaction depends on the electronegativity of the substituents on the silyl ligand [3]. The three electron-donating alkyl groups on the silicon atom of **24** lengthen the Rh–Si bond.

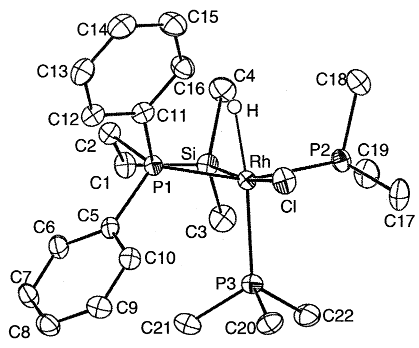

Fig. 1. ORTEP drawing of $RhH(Cl))(\eta^2\text{-}Me_2SiCH_2CH_2PPh_2)(PMe_3)_2$ (**23**).

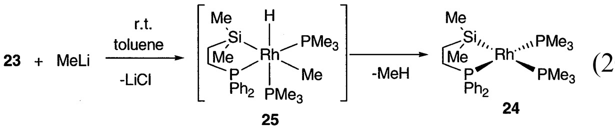

(20)

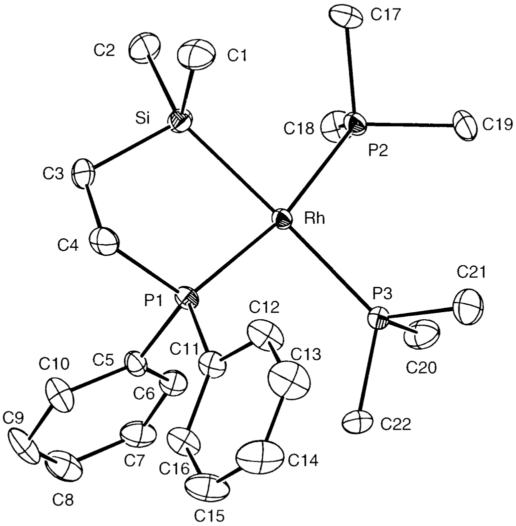

Fig. 2. ORTEP drawing of $Rh(\eta^2\text{-}Me_2SiCH_2CH_2PPh_2)(PMe_3)_2$ (**24**).

Complex **24** is fluxional in $C_6D_5CD_3$. At − 40 °C, the ^{31}P-NMR signal of the two PMe_3 ligands appear nonequivalently at − 21.1 ppm (apparent dt, $^1J(PRh) = 112.9$ Hz, $^2J(PP\mathit{cis}) = 35.9$ Hz, PMe_3 *trans* to Si) and − 9.0 ppm (ddd, $^2J(PP\mathit{trans}) = 296.0$ Hz,

^1J(PRh) = 148.0 Hz, ^2J(PP*cis*) = 36.6 Hz, PMe_3 *cis* to Si). The PPh_2 signal appears at 70.5 ppm (ddd, ^2J(PP*trans*) = 296.0 Hz, ^1J(PRh) = 157.2 Hz, ^2J(PP*cis*) = 35.1 Hz). The coupling pattern is consistent with the geometry as illustrated in Fig. 2. At 20 °C, only a single signal appears for the two PMe_3 ligands equivalently at − 14.8 ppm as a slightly broad triplet (^1J(PRh) = ^2J(PP) = 129.7 Hz), and the ^{31}P resonance of the PPh_2 moiety appears at 70.4 ppm as double triplets coupled with the ^{103}Rh and ^{31}P nuclei of the two PMe_3 ligands (^1J(PRh) = 160.2 Hz, ^2J(PP) = 131.2 Hz). These spectroscopic features are consistent with the occurrence of intramolecular exchange process of two PMe_3 ligands on the NMR timescale.

When an excess of MeLi exists in a toluene solution of **24**, disproportionation takes place to afford the coordinatively saturated silylrhodium(I) complex Rh(η^2-$Me_2SiCH_2CH_2PPh_2$)$(PMe_3)_3$ (**26**) and unidentified product(s) (Eq. (21)). Treatment of **23** with MeLi in the presence of PMe_3 afforded **26** in 74% yield (Eq. (22)) [20]. Complex **26** is much more stable than the unsaturated complex **24**. The X-ray crystal structure study shows that **26** adopts a trigonal-bipyramidal geometry in which the silyl and PMe_3 ligands occupy the axial position (Fig. 3). Complex **26** exhibits dynamic behavior in the solution state. The $^{31}P\{^1H\}$-NMR spectrum at − 30 °C shows three signals at − 22.8 ppm [ddd, ^1J(PRh) = 154.3 Hz, ^2J(PP) = 116.3, 47.4 Hz, two equatorial PMe_3], − 13.1 ppm [apparent dq, ^1J(PRh) = 94.8 Hz, ^2J(PP) = 48.1 Hz, axial PMe_3], and 65.7 ppm [ddt, ^1J(PRh) = 159.0 Hz, ^2J(PP) = 116.3, 48.8 Hz, PPh_2]. In the $^{31}P\{^1H\}$-NMR at 50 °C, the signals of the three PMe_3 ligands appear equivalently at − 22.3 ppm. The ^{31}P resonance of the PPh_2 moiety at 50 °C appears at 66.1 ppm as a slightly broad doublet coupled with the ^{103}Rh nuclei (^1J(PRh) = 150.6 Hz) in which the coupling with the PMe_3 ligands is no longer observed. This implies the existence of an intermolecular exchange process with the PMe_3 ligands. A variable temperature ^{31}P-NMR study on a mixture of **26** and PMe_3 in $C_6D_5CD_3$ revealed that respective signals assignable to axial, equatorial, and free PMe_3 appear separately and sharply at − 30 °C, but when the temperature is raised, they gradually broaden and finally coalesce at 50 °C. The observations imply that complex **26** serves as a convenient precursor for generating a highly reactive 16e silylrhodium(I) complex **24** via dissociation of a PMe_3 ligand (Eq. (23)).

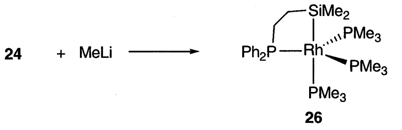

(21)

$$23 + \text{MeLi} + \text{PMe}_3 \xrightarrow[\text{-Li-Cl}\ \text{-MeH}]{\text{r.t. toluene}} 26 \qquad (22)$$

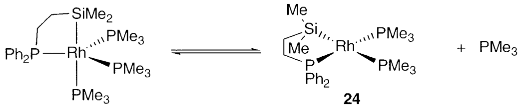

(23)

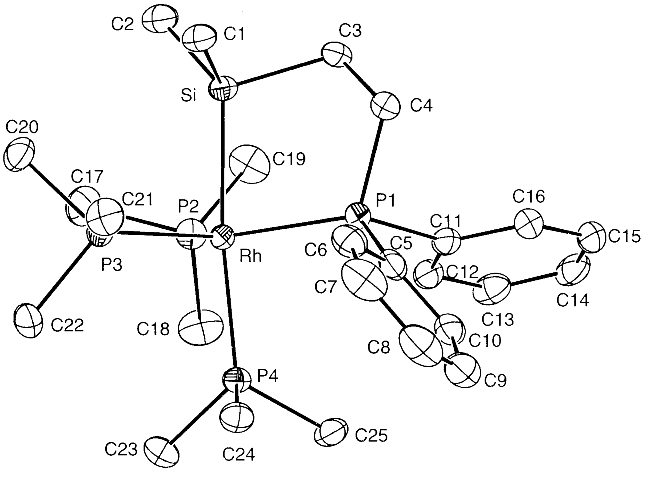

Fig. 3. ORTEP drawing of Rh(η^2-$Me_2SiCH_2CH_2PPh_2$)$(PMe_3)_3$ (**26**).

Complex **24** represents the first example of a coordinatively unsaturated trialkylsilylrhodium(I) complex. This complex is expected to be highly reactive toward various small molecules due to the strongly electron-releasing character of the trialkylsilyl moiety.

In fact, reaction of **24** with an excess of $HSiMe_2Ph$ proceeds at r.t. to give a Si–H oxidative addition product *fac*-[Rh(H)($SiMe_2Ph$)(η^2-$Me_2SiCH_2CH_2PPh_2$)-$(PMe_3)_2$] (**27**) [17]. Further reaction takes place at r.t. to afford a 1:1 mixture of the dihydrido complex *fac*-[RhH_2\{η^2-$Me_2SiCH_2CH_2PPh_2$\}$(PMe_3)_2$] (**28**) and $(SiMe_2Ph)_2$ in 91% yield each. Dihydrido complex **28** can be independently synthesized by the treatment of **23** with $LiAlH_4$ in THF (Eq. (25)) and is characterized based on the results of elemental analysis and various spectroscopic data. Scheme 1 illustrates a plausible mechanism for the formation of **28** and $(SiMe_2Ph)_2$, although the σ-bond metathesis type reaction cannot be ruled out. The first step is the dissociation of PMe_3 from **27** and then the oxidative addition of $HSiMe_2Ph$ takes place to give a silylrhodium(V) intermediate **29**. The similar silylrhodium(V) complex has been reported by Nagashima et al. [21]. Complex **29** undergoes reductive elimination of the disilane and ligation of PMe_3 to give **28** (Eq. (24)).

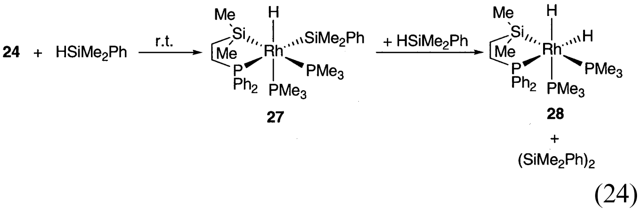

(24)

$$23 + \text{LiAlH}_4 \rightarrow 28 \qquad (25)$$

When the reaction of $RhCl(PMe_3)_3$ with $HSiAr_3$ is carried out at r.t., a Si–H oxidative addition product *mer*-$[RhCl(H)(SiAr_3)(PMe_3)_3]$ (**30**) is formed (Eq. (26)) [22]. In the reaction, $RhCl(H)_2(PMe_3)_3$ and $(SiAr_3)_2$ derived from the Si–Si reductive elimination were not detected. The dramatic difference of reactivity between **27** and **30** is of great interest. The difference is attributable to the exceptionally strong *trans*-effect of the silyl ligand in **27**. Further reaction of **27** requires the dissociation of the phosphine ligand, to form the bis(silyl)rhodium(V) intermediate. In complex **27**, the silyl group of (2-phosphinoethyl)silyl chelate ligand would accelerate the dissociation of the *trans*-PMe_3 ligand, while such an effect is not operative in complex **30**.

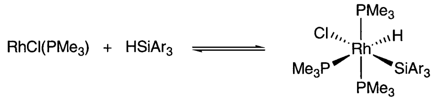

30

(26)

The iridium analog of **23** *mer*-$[IrCl(H)\{\eta^2\text{-}Me_2SiCH_2CH_2PPh_2\}(PMe_3)_2]$ (**31**) can be readily prepared by the thermal reaction of the cationic iridium(I) complex $[Ir(CO)(PMe_3)_4]Cl$ with $Ph_2PCH_2CH_2SiMe_2H$ in toluene at 80 °C (Eq. (27)) [23].

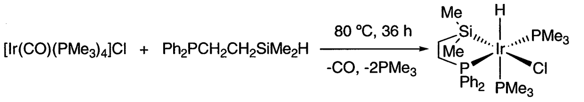

31

(27)

Addition of MeLi to **31** in toluene results in the formation of hydrido(methyl)iridium(III) complex **32** as a thermally stable form at r.t. (Eq. (28)) [23]. The ^1H-, ^{13}C-, ^{29}Si-, and ^{31}P-NMR data established that **32** possess hydrido, methyl, and silyl ligands in a *mer* configuration. In the complex *fac*-$IrH(Me)(SiR_3)(PMe_3)_3$ reported previously by Aizenberg and Milstein, a strongly *trans*-influencing silyl ligand is located *trans* to the PMe_3 ligand [24]. In contrast, surprisingly, the silyl ligand in **32** is located *trans* to the strongly *trans*-influencing methyl ligand. As mentioned above, the reaction of $RhH(Cl)(\eta^2\text{-}Me_2SiCH_2CH_2PPh_2)(PMe_3)_2$ with MeLi did not give the rhodium analog of **32** $RhH(Me)(\eta^2\text{-}Me_2SiCH_2CH_2PPh_2)(PMe_3)_2$ but gave $Rh(\eta^2\text{-}Me_2SiCH_2CH_2PPh_2)(PMe_3)_2$ accompanied by the reductive elimination of MeH. The difference of the thermal stability between rhodium and iridium is consistent with the general trend that the iridium complex with high oxidation state is more stable than the corresponding rhodium complex [25].

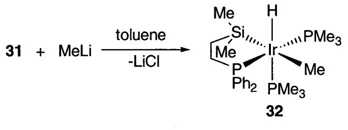

32

(28)

Thermolysis of **32** in C_6D_6 at 50 °C for 36 h gives a geometric isomer **33** as a main product, in which silyl, hydrido, and methyl ligands are located at a *fac* configuration (Eq. (29)) [26]. To our knowledge, this is a very rare example of the geometric isomerization of the hydrido(alkyl) complexes. Further heating of the resulting solution at 80 °C leads to orthometalation to give **34**. The exceptionally high thermal stability of **32** and **33** against reductive elimination of methane is attributable to the electron-richness of the metal center resulting from the ligation of the electron-releasing silyl and phosphine ligands.

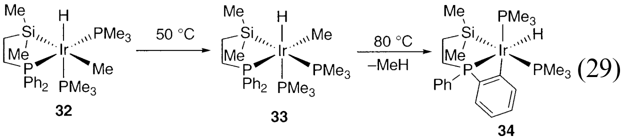

(29)

Treatment of **32** with 1 equiv. H_3SiR (R = *n*-butyl, pentyl, or hexyl) at 45 °C leads to the almost exclusive formation of $IrH_2\{\eta^2\text{-}Me_2SiCH_2CH_2PPh_2\}(PMe_3)_2$ (**35**) and H_2SiMeR within 1 h (Eq. (30)) [27]. Aizenberg and Milstein reported that when $[IrMe(H)(SiEt_3)(PMe_3)_3]$ was heated to 100 °C not only C–H but also Si–C reductive elimination occurred to give CH_4 and $SiMeEt_3$. The ratio of CH_4 to $SiMeEt_3$ was ca. 4:1 [24]. Our reaction is the first clean transformation of an alkyl(hydrido)silyl complex into a silicon-containing organic product. A conventional mechanism involving

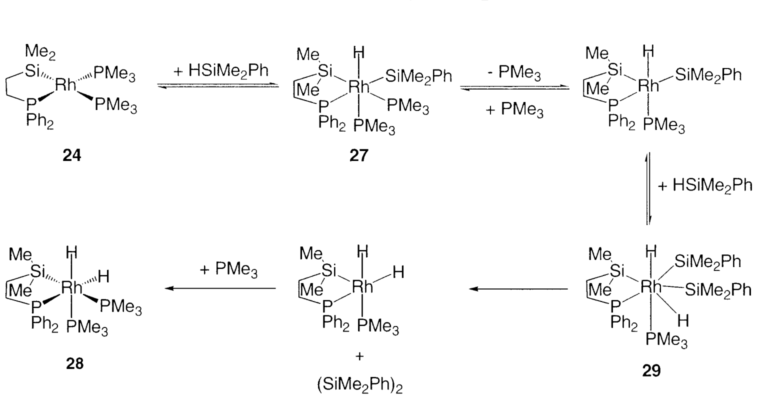

Scheme 1. Formation mechanism of $RhH_2(\eta^2\text{-}Me_2SiCH_2CH_2PPh_2)(PMe_3)_2$ (**28**) and $(SiMe_2Ph)_2$.

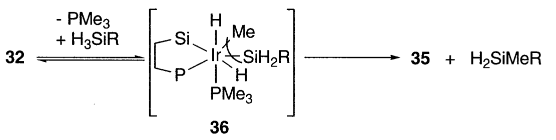

Scheme 2. Formation mechanism of $IrH_2(\eta^2\text{-}Me_2SiCH_2CH_2PPh_2)(PMe_3)_2$ (**35**) and H_2SiMeR involving oxidative addition/reductive elimination process.

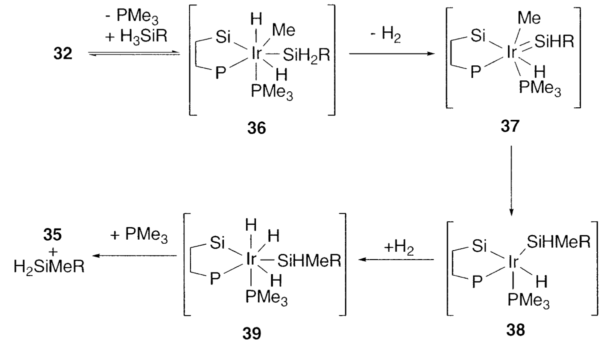

Scheme 3. Formation mechanism of $IrH_2(\eta^2\text{-}Me_2SiCH_2CH_2PPh_2)(PMe_3)_2$ (**35**) and H_2SiMeR involving a silylene intermediate.

oxidative addition/reductive elimination can be a candidate to explain the reaction in Eq. (30), as illustrated in Scheme 2. According to Scheme 2, carbon-silicon reductive elimination has to occur preferentially over carbon–hydrogen reductive elimination. This assumption is in contradiction to the usual tendency of reductive elimination, although we cannot rule out this mechanism [28].

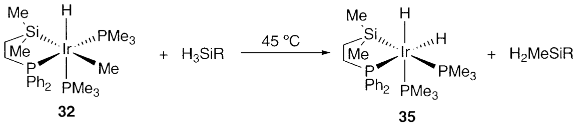

(30)

(R = *n*-butyl, pentyl, or hexyl)

An alternative mechanism proposed by us is illustrated in Scheme 3. This mechanism involves the initial generation of a seven-coordinate iridium(V) intermediate **36** by dissociation of a PMe_3 ligand and subsequent Si–H oxidative addition. Similar seven-coordinate trihydridobis(silyl)iridium(V) [29] and -rhodium(V) [21] complexes have been reported. The intermediate **36** eliminates dihydrogen to give a methyl(silylene) intermediate **37** which undergoes 1,2-shift of the Me ligand to the silylene silicon atom to give a hydrido(methylsilyl)iridium(III) complex **38**. Berry et al. reported the facile migration of a silyl ligand from tantalum to a carbene carbon atom at − 10 °C [30]. Very recently, Ozawa et al. reported that *cis*-$PtR(SiHPh_2)(PMe_2Ph)_2$ was converted to *cis*-$PtH(SiRPh_2)(PMe_2Ph)_2$ at r.t. in C_6D_6. In their proposed mechanism, the first step is the dissociation of PMe_2Ph, followed by 1,2-H-shft from a silyl silicon atom to a platinum center. The resulting $PtH(R)(PMe_2Ph)({=}SiPh_2)$ undergoes 1,2-R-shift from platinum to the silylene silicon atom and subsequent ligation of PMe_2Ph to afford *cis*-$PtH(SiRPh_2)(PMe_2Ph)_2$ [31]. Oxidative addition of H_2 to **38** gives a seven-coordinate iridium(V) species **39**, which subsequently eliminates H_2MeSiR and binds PMe_3 to give **35**. We carried out the thermal reaction of **32** with a monohydrosilane $HSiMe_2{}^{p}Tol$ from which it is impossible to generate a silylene moiety via dehydrogenation as illustrated in Scheme 3. In contrast to the reaction with trihydrosilanes in Eq. (30) (at 45 °C, 1 h), the reaction with $HSiMe_2{}^{p}Tol$ is extremely slow at 45 °C. At 55 °C, the reaction proceeds almost quantitatively to give $Ir(H)(SiMe_2{}^{p}Tol)\{\eta^2\text{-}Me_2Si(CH_2)_2PPh_2\}(PMe_3)_2$ (**40**) and methane within 6 h (Eq. (31)). The Si–C bond formation product ($Me_3Si^{p}Tol$) and **35** were not detected spectroscopically. These results indicate that the rate-determining step of the reaction in Eq. (31) needs a more drastic condition than that given in Eq. (30), but even under the conditions (55 °C, 6 h) Si–C reductive elimination does not occur at all. These observations favor the mechanism given in Scheme 3 involving the silylene intermediate **37** for the metal-mediated silicon–carbon bond formation reaction. This stoichiometric reaction is applicable to the elusive transition-metal catalyzed hydrosilane–alkane dehydrogenative coupling reactions (Eq. (32)).

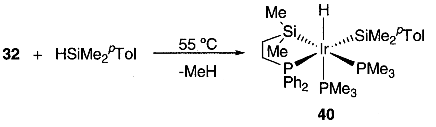

(31)

$$R^1\text{-H} + \text{H-SiR}^2_3 \xrightarrow[\text{-H}_2]{[M]} R^1\text{-SiR}^2_3 \qquad (32)$$

When the thermal reaction of **32** at 60 °C is carried out in the presence of PMe_3, the coordinatively saturated silyliridium(I) complex $Ir(\eta^2\text{-}Me_2SiCH_2CH_2PPh_2)(PMe_3)_3$ (**41**) is formed almost quantitatively (Eq. (33)) [23]. The five-coordinate complex **41** is fluxional in $C_6D_5CD_3$ at r.t. In the ^1H-NMR spectrum at − 60 °C, the signals of one axial and two equatorial PMe_3 ligands appear nonequivalently. At 50 °C, these signals become equivalent to be a very broad singlet. At 80 °C, the ^{31}P resonance of the PPh_2 moiety appears as a broad quartet coupled with the ^{31}P nuclei of the three PMe_3 ligands ($J(PP) = 79$ Hz), which is consistent with the existence of the intramolecular exchange of the three PMe_3 ligands. It has been known that a methyliridium(I) complex $Ir(Me)(PMe_3)_4$ exhibits intramolecular exchange of PMe_3 ligands [32a,b]. In contrast, the rhodium analogs $Rh(\eta^2\text{-}Me_2SiCH_2CH_2PPh_2)(PMe_3)_3$ (**26**) and $RhMe(PMe_3)_4$ [32c] exhibit the intermolecular exchange of the PMe_3 ligands.

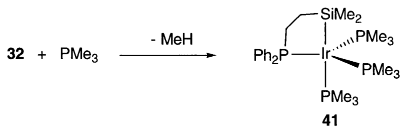

(33)

The ORTEP drawing of **41** is shown in Fig. 4. Complex **41** adopts a five-coordinate, slightly distorted trigonal-bipyramidal arrangement in which the silicon atom and a PMe_3 ligand occupy the axial positions while the PPh_2 moiety and the two PMe_3 ligands are located in the equatorial sites. The Ir–Si bond length (2.447(5) Å) lies in the normal range and is close to those of the silyliridium(I) complexes, Ir(η^2-$PPh_2CH_2CH_2SiMe_2$)(PPh_3)$(CO)_2$ (2.454(6) Å) [12] and $IrSiMe_2Ph(CO)_2(PMe_3)_2$ (2.442(3) Å) [33], reported earlier. The Ir–P (PPh_2) bond length (2.279(5) Å) of **41** is shorter than that of $Ir(PPh_2CH_2CH_2SiMe_2)(PPh_3)(CO)_2$ (2.342(5) Å) [12]. This indicates that the back donation from the iridium center to the phosphorus atom in the former is more effective than that in the latter because of the more electron rich metal center in the former.

To investigate the lability of PMe_3 ligands in Ir(η^2-$Me_2SiCH_2CH_2PPh_2$)$(PMe_3)_3$ (**41**), 5 equiv. $P(CD_3)_3$ were vacuum-transferred into the C_6D_6 solution of **41** [23]. Instantly, the intensity of the ^{1}H-NMR signal of PMe_3 ligands in **41** started decreasing at r.t. and the signal of free PMe_3 increased compensating the decrease of the signals of PMe_3 ligands. The observation is consistent with the facile generation of a 16e silyliridium(I) complex Ir(η^2-$Me_2SiCH_2CH_2PPh_2$)$(PMe_3)_2$ (**42**) from complex **41** even at r.t. Recently, in several laboratories, attention has been paid to isolate the unsaturated four-coordinate silyliridium(I) complexes, although their isolation has not been successful yet. Aizenberg and Milstein reported that thermolysis of *fac*-$(Me_3P)_3Ir(Me)(H)(SiPh_3)$ in C_6D_6 under relatively severe conditions (100 °C for 24 h) led to the formation of the *ortho*-metalated product $(Me_3P)_3Ir\{(C_6H_4)SiPh_2\}(H)$, and they assumed that a 16e silyliridium(I) complex $(Me_3P)_3Ir(SiPh_3)$ is generated as a key intermediate by methane reductive elimination [24]. A 16e silyliridium(I) complex $Ir\{Si(SiMe_3)_3\}(PMe_3)_3$ has been spectroscopically detected in solution at −80 °C by Tilley et al. [34] (Fig. 5).

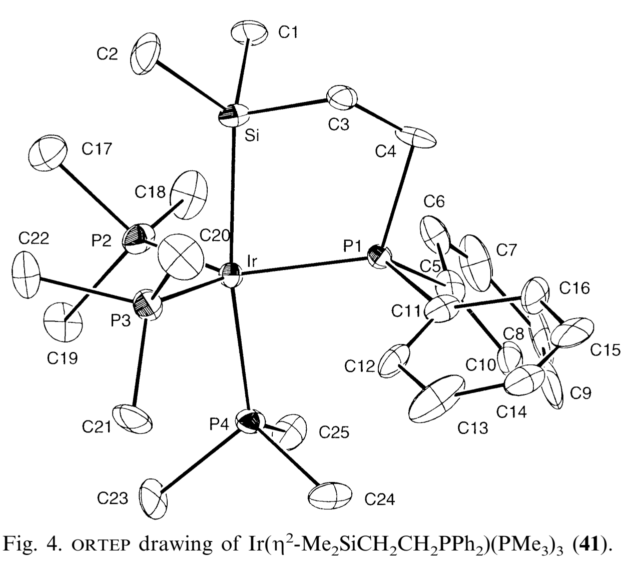

Fig. 4. ORTEP drawing of Ir(η^2-$Me_2SiCH_2CH_2PPh_2$)$(PMe_3)_3$ (**41**).

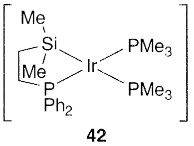

42

Fig. 5. A 16e silyliridium(I) complex Ir(η^2-$Me_2SiCH_2CH_2PPh_2$)-$(PMe_3)_2$ (**42**).

When reaction of **41** with 5 equiv. $HPhMeSiSiMe_3$ is performed at r.t., *fac*-[IrH($SiMe_2SiMe_2Ph$)(η^2-$Me_2SiCH_2CH_2PPh_2$)$(PMe_3)_2$] (**43**) is formed via the rearrangement of substituents on a disilanyl ligand (Eq. (34)) [35]. A small amount of $HMe_2SiSiMe_2Ph$ was also detected spectroscopically. The formation of *fac*-[IrH($SiMePhSiMe_3$)(η^2-$Me_2SiCH_2CH_2PPh_2$)$(PMe_3)_2$] (**44**), a simple oxidative addition product, was confirmed in the course of the reaction, but **44** finally disappeared. Further, thermolysis of this solution at 45 °C caused the rearrangement of hydrodisilane to give an isomeric mixture of $HPhMeSiSiMe_3$ and $HMe_2SiSiMe_2Ph$. After five days, the molar ratio of $HPhMeSiSiMe_3$ to $HMe_2SiSiMe_2Ph$ became 2:3, and **43** finally decomposed. Reaction of **41** with $HMe_2SiSiMe_2Ph$ was carried out under the same conditions, which resulted in the formation of a mixture of $HPhMeSiSiMe_3$ and $HMe_2SiSiMe_2Ph$ in the ratio of 2:5. The formation and decomposition of **43** was also confirmed spectroscopically. Each reaction led to the isomeric mixture of hydrodisilane in a different ratio. This means that the active catalyst **43** decomposed before achieving the equilibrium. This isomerization reaction can be explained by the mechanism shown in Scheme 4. The first step is the dissociation of PMe_3, followed by oxidative addition of $HPhMeSiSiMe_3$. The resulting disilanyliridium(III) complex **44** undergoes dissociation of PMe_3 and 1,2-shift of the $SiMe_3$ group to generate a silyl(silylene) intermediate **45** which is converted to its isomer **46** via 1,3-Me-shift [36]. The silyl(silylene) intermediate **46** leads to 1,2-silyl-shift and coordination of PMe_3 to afford **43**. Intermediate **43** eliminates an isomeric hydrodisilane and the resulting iridium part ligates PMe_3 to give **41**.

To detect the silyl-silylene intermediate in Scheme 4, $HMe(MeO)SiSiMe_3$ was used in place of $HPhMeSiSiMe_3$ [35]. Thermolysis of **41** in the presence of $HMe(MeO)SiSiMe_3$ leads to the clean formation of

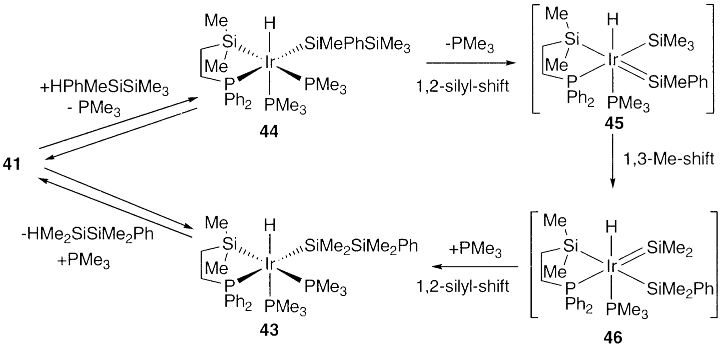

Scheme 4. Mechanism for isomerization of disilane via silyl(silylene) intermediates.

47 (Eq. (35)) [37]. The geometry of **47** can be uniquely determined by the NMR data. In the ^{29}Si-NMR spectrum, the signals of two silylene ligands appeared nonequivalently at 62.8 ppm (dd, J(SiP*trans*) = 135.9 Hz, J(SiP*cis*) = 11.8 Hz) and 63.1 ppm (dd, J(SiP*trans*) = 136.9 Hz, J(SiP*cis*) = 13.0 Hz), which are shifted significantly downfield from those of previously reported silyliridium compounds [23,27,38,39]. The formation of **47** strongly supports the mechanism for the hydrodisilane isomerization shown in Scheme 4 which involves the 1,3-Me-shift on silyl(silylene) intermediates.

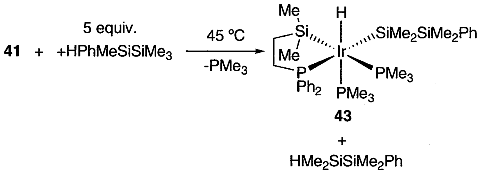

(34)

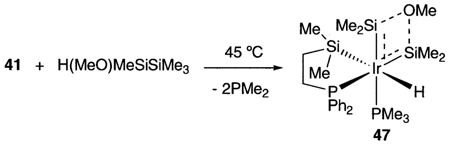

(35)

Alkyl(hydrido)iridium(III) complexes **49** and **50** with η^2-MesHSiCH$_2$CH$_2$PPh$_2$ (Mes = 2,4,6-C$_6$H$_2$Me$_3$) have been synthesized as illustrated in Eq. (36) [38,39]. Thermolysis of these alkyl(hydrido) complexes results in generation of a coordinatively unsaturated silyliridium(I) complex **51** via elimination of alkane to give the intramolecular C–H bond activation products **52** and **53** (Eq. (37)). Complexes **49** and **50** react with MeOH at 60 °C to give a dihydrido(methoxysilyl)iridium(III) complex **54** (Eq. (38)). Formation of the corresponding alkane was confirmed by ^{1}H-NMR spectroscopy. The reaction can be rationalized by the mechanism involving the silylene complex **55** generated via 1,2-H-shift from the silyl silicon atom to the coordinatively unsaturated iridium(I) center (Scheme 5). MeOH attacks the silylene silicon atom of **55** nucleophilically to afford **54**. MeOH has been known to be an effective trapping agent for silylene complexes, since the M=Si bond is fairly polarized in the M$^{\delta-}$–Si$^{\delta+}$ fashion [40]. Introduction of a methoxy group to the silicon atom is most likely to give evidence for the facile migration of hydrogen from the silyl silicon atom to the iridium center.

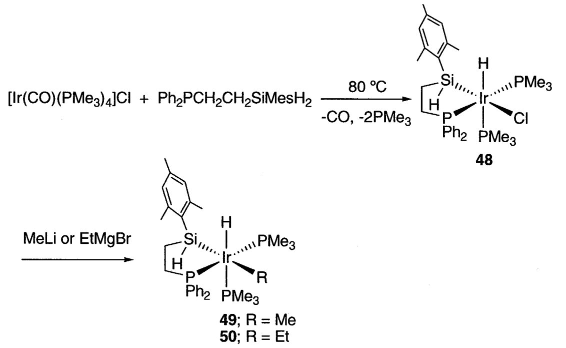

(36)

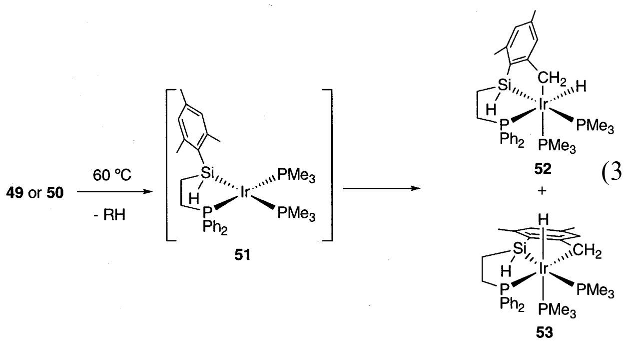

(37)

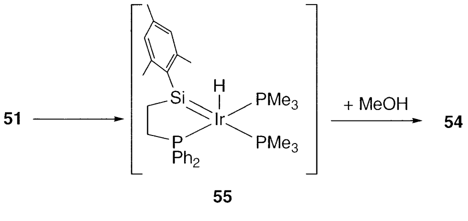

Scheme 5. Formation mechanism of **54** involving a silylene intermediate.

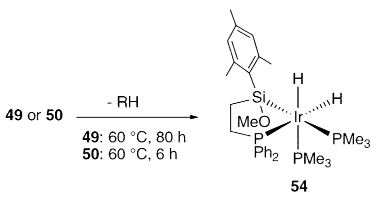

(38)

3.3. Ru and Os complexes

Stobart et al. reported that heating of the THF solution of $Ph_2PCH_2CH_2SiMe_2H$ and $M_3(CO)_{12}$ (M = Ru, Os) in a sealed tube afforded the octahedral M(II) complexes $[M(\eta^2\text{-}Me_2SiCH_2CH_2PPh_2)_2(CO)_2]$ (**56**; M = Ru, **57**; M = Os) (Eq. (39)) [41]. The geometry of these complexes has been confirmed by spectroscopic data and X-ray diffraction study.

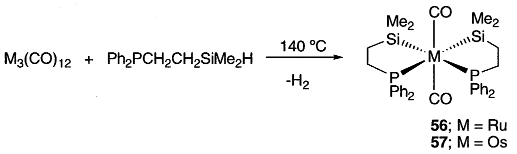

(39)

3.4. Mn and W complexes

Schubert et al. showed that (phosphinoethyl)hydrosilane is a good ligand precursor for the silane σ-complex. $(\eta^5\text{-}C_5H_4Me)Mn(CO)_3$ and $W(CO)_6$ reacted with $Ph_2PCH_2CH_2SiHR_2$ (R = Me, Ph) upon photolysis to give the η^2-silane complexes (Eq. (40) and (41) in Refs. [42] and [43], respectively).

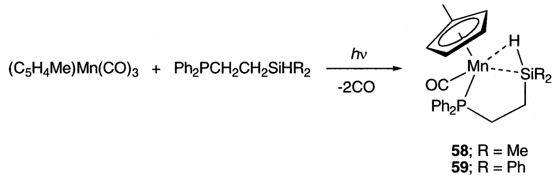

(40)

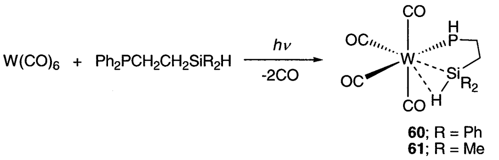

(41)

4. Synthesis of η^2-(phosphinomethyl)silyl complexes

(Phosphinomethyl)silyl fragment can work not only as a bidentate chelate-type ligand (**A**) but also as an unsymmetrical bridging ligand to a bimetallic system (**B**) (Fig. 6).

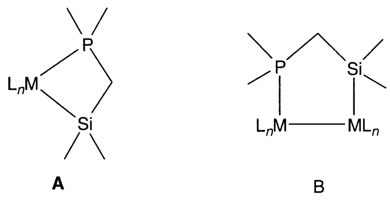

Fig. 6. Coordination modes of (phosphinomethyl)silyl ligands.

Stobart et al. reported the thermal reaction of $Ru_3(CO)_{12}$ with $HMe_2SiCH_2PPh_2$ to give a ruthenium dinuclear complex **62** (Eq. (42)) [44]. The structure of **62** has been determined by X-ray crystal structural analysis. Complex **62** is a symmetrical dimer in which two (phosphinomethyl)silyl liagnds bridge two ruthenium atoms. In this reaction, formation of the mononuclear complex with η^2-(phosphinomethyl)silyl chelate ligands was not observed. The osmium analog **63** is also obtained by the reaction of $Os_3(CO)_{12}$ with $HMe_2SiCH_2PPh_2$ (Eq. (42)) [44].

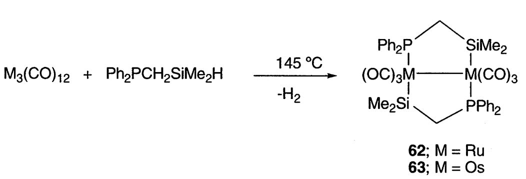

(42)

In contrast to the five-membered (2-phosphinoethyl)silyl complexes, there are few examples of four-membered η^2-(phosphinomethyl)silyl complexes. The mononuclear complex $IrH_2(\eta^2\text{-}Me_2SiCH_2PPh_2)(CO)(PPh_3)$ (**64**) with the η^2-(phosphinomethyl)silyl chelate ligand has been synthesized by the reaction of an iridium(I) complex with $HMe_2SiCH_2PPh_2$ (Eq. (43)) [7]. Treatment of $IrH(CO)(PPh_3)_3$ with $HMe_2SiCH_2PPh_2$ at r.t. causes the oxidative addition of the Si–H bond and coordination of the phosphine moiety to the same metal center to afford **64** in 59% isolated yield. The ORTEP drawing of **64** is shown in Fig. 7. The two

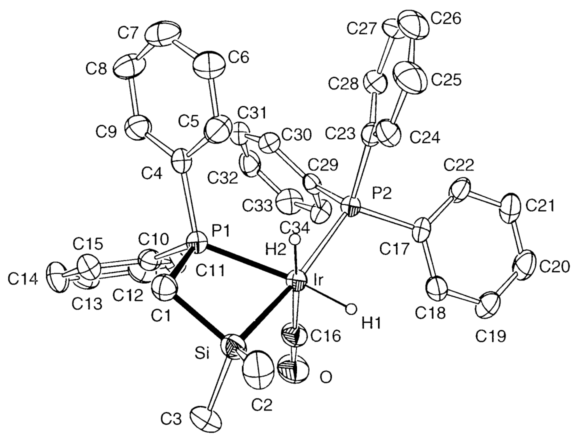

Fig. 7. ORTEP drawing of $IrH_2(\eta^2\text{-}Me_2SiCH_2PPh_2)(CO)(PPh_3)$ (**64**).

hydrogen atoms attached to the iridium center were located by the difference Fourier synthesis and refined isotropically. Coordination geometry around iridium is a distorted octahedron. Strongly *trans*-influencing silyl and two hydrido ligands are located in *fac*-relationship. The P1–Ir–Si bite angle is 71.07(9)°. The corresponding bite angles for the five-membered (2-phosphinoethyl)silyl chelate ligands lie in the 80–84° range [8–12,14,17,20,23]. The NMR and IR spectral data are consistent with the crystal structure of **64**. Further treatment of $IrH_2(\eta^2\text{-}Me_2SiCH_2PPh_2)(CO)(PPh_3)$ (**64**) with $HMe_2SiCH_2PPh_2$ affords a bis(phosphinomethylsilyl)iridium(III) complex *cis*-$IrH(\eta^2\text{-}Me_2SiCH_2PPh_2)_2$-(CO) (**65**) in 23% isolated yield (Eq. (44)) [7]. The NMR and IR data established the geometry of **65** in which two chemically equivalent phosphinomethylsilyl ligands are coordinated to the iridium(III) center in η^2-fashion. The $^{31}P\{^1H\}$-NMR spectrum shows a singlet at -44.1 ppm. The $^{29}Si\{^1H\}$-NMR spectrum shows a dd pattern ($J = 103.1$, 46.5 Hz) due to virtual couples (AA′XX′). The Si–P coupling constants are consistent with the *cis*-geometry. In the ^1H-NMR spectrum, the signal of IrH appears at -7.78 as a triplet ($^2J(HP\mathit{cis}) = 19.2$ Hz). The IR spectrum shows two strong bands at 1934 and 2033 cm^{-1} that are assigned to the terminal CO and IrH stretching vibrations, respectively.

Schubert et al. reported the formation of the square planar platinum(II) complex *cis*-$Pt(\eta^2\text{-}Me_2SiCH_2PPh_2)$-$(SiPh_3)(PPh_3)$ (**66**) by the reaction of $Ph_3SiMe_2SiCH_2$-PPh_2 with $Pt(C_2H_4)(PPh_3)_2$ via oxidative addition of the Si–Si bond (Eq. (45)). The P–Pt–Si bite angle is 70.65(5)°, which is quite similar to that in **64** [11].

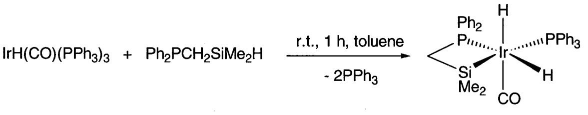

(43)

64

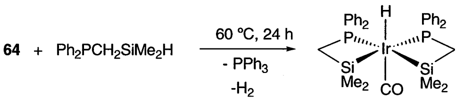

(44)

65

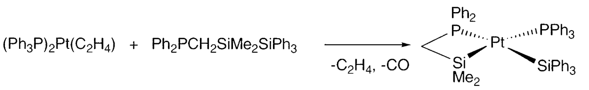

(45)

66

The reactivity and catalytic performance of organotransition-metal complexes depend on the ligand environment of the metal. Over the last few years, much effort has been made to clarify the influence of specific geometries of ligands on the reactivity of the metal centers. Theoretical and experimental results indicate that in the platinum(0) $Pt(PR_3)_2$ system the smaller the P–Pt–P bite angle the higher the reactivity towards oxidative addition reactions [45]. The four-membered (phosphinomethyl)silyl ligand enforces the bite angle (P–Ir–Si) around 70°. The influence of the bite angle in the phosphinoalkylsilyl ligand $[\eta^2\text{-}Me_2Si(CH_2)_nPPh_2$, $n = 1,2]$ on the reactivity of transition metal complexes is of great interest.

5. Conclusion

It has been assumed over the recent decades that the introduction of silyl groups as supporting ligands could change or enhance the catalytic performance of soluble transition metal complexes due to the electron-releasing character and strong *trans*-influence ability of these silyl ligands. However, the facile cleavage of silyl ligands has retarded such an application. To suppress the elimination of silyl ligands, chelate-type (phosphinoalkyl)silyl lignds may be employed. η^2-(Phosphinoalkyl)silyl complexes have been synthesized mainly by the reaction of unsaturated metal complexes with the corresponding ligand precursor (phosphinoalkyl)silane $R_2P(CH_2)_n$-SiR_2H via coordination of the phosphine moiety and oxidative addition of the Si–H part. In reactions of metal complexes with $R_2P(CH_2)_2SiR_2H$, the five-membered η^2-(phosphinoethyl)silyl complexes are formed. In contrast (phosphinomethyl)silyl group functions not only as a four-membered chelate-type ligand but also as an unsymmetrical bridging ligand over the two transition-metal centers. This paper has reviewed the investigations on (phosphinoalkyl)silyl complexes, most of which have dealt with only syntheses and structures. However, the unusual reactivities of these complexes have been gradually disclosed through these studies: The (phosphinoethyl)silyl ligand is efficient for controlling the elimination of silyl ligands from the metal centers. The (phosphinoethyl)silyliridium complexes promoted the silicon–carbon bond formation via a 1,2-Me-shift to the silylene silicon atom and rearrangement of substituents on hydrodisilanes. The (phosphinoethyl)silylrhodium complex mediated the dehydrogenative coupling of monohydrosilanes. These novel reactivities seem to result from the electron-releasing and strong *trans* effect character of the silyl ligands. The introduction of these (phosphinoethyl)silyl ligands is expected to open up some rich new chemistry.

Acknowledgements

The authors wish to thank Nissan Science Foundation and Inoue Foundation for Science for financial supports.

References

[1] (a) J. Chatt, C. Eaborn, S. Ibekwe, J. Chem. Soc. Chem. Commun. (1966) 700;
(b) R. McWeeny, R. Mason, A.D.C. Towl, Discuss. Faraday Soc. 47 (1969) 20;
(c) R.N. Haszeldine, R.V. Parish, J.H. Setchfield, J. Organomet. Chem. 57 (1973) 279;
(d) H. Tobita, K. Hasegawa, J.J.G. Minglana, L.-S. Luh, M. Okazaki, H. Ogino, Organometallics 18 (1999) 2058.

[2] M. Aizenberg, D. Milstein, Science 265 (1994) 359.

[3] T.D. Tilley, in: S. Patai, Z. Rappoport (Eds.), The Chemistry of Organic Silicon Compounds, Wiley, New York, 1989, p. 1415.

[4] J. Grobe, U. Möller, J. Organomet. Chem. 17 (1969) 263.

[5] R.D. Holmes-Smith, R.D. Osei, S.R. Stobart, J. Chem. Soc. Perkin Trans. (1983) 861.

[6] (a) N.E. Schore, L.S. Benner, B.E. LaBelle, Inorg. Chem. 20 (1981) 3200;
(b) N.E. Schore, L.S. Benner, J. Org. Chem. 46 (1981) 2306.

[7] M. Okazaki, M. Iwata, H. Ogino, The 49th Symposium on Coordination Chemistry of Japan, Sapporo, Abstract 2P9-D12, 1999.

[8] R.D. Holmes-Smith, S.R. Stobart, T.S. Cameron, K. Jochem, J. Chem. Soc. Chem. Commun. (1981) 937.

[9] S.L. Grundy, R.D. Holmes-Smith, S.R. Stobart, M.A. Williams, Inorg. Chem. 30 (1991) 3333.

[10] M. Murakami, T. Yoshida, S. Kawanami, Y. Ito, J. Am. Chem. Soc. 117 (1995) 6408.

[11] H. Gilges, G. Kickelbick, U. Schubert, J. Organomet. Chem. 548 (1997) 57.

[12] M.J. Auburn, R.D. Holmes-Smith, S.R. Stobart, J. Am. Chem. Soc. 106 (1984) 1314.

[13] M.J. Auburn, S.R. Stobart, Inorg. Chem. 24 (1985) 318.

[14] M. Murakami, T. Yoshida, Y. Ito, Chem. Lett. (1996) 13.

[15] M.J. Auburn, S.L. Grundy, S.R. Stobart, M.J. Zaworotko, J. Am. Chem. Soc. 107 (1985) 266.

[16] F.L. Joslin, S.R. Stobart, J. Chem. Soc. Chem. Commun. (1989) 504.

[17] M. Okazaki, S. Ohshitanai, H. Tobita, H. Ogino, submitted for publication.

[18] D.L. Thorn, R.L. Harlow, Inorg. Chem. 29 (1990) 2017.

[19] D.L. Lichtenberger, A. Rai-Chaudhuri, J. Am. Chem. Soc. 113 (1991) 2923.

[20] M. Okazaki, S. Ohshitanai, H. Ogino, The 50th Symposium on Coordination Chemistry of Japan, Kusatsu, Abstract 1D-D10, 2000.

[21] H. Nagashima, K. Tatebe, T. Ishibashi, A. Nakaoka, J. Sakakibara, K. Itoh, Organometallics 14 (1995) 2868.

[22] K. Osakada, S. Sarai, T. Koizumi, T. Yamamoto, Organometallics 16 (1997) 3973.

[23] M. Okazaki, H. Tobita, H. Ogino, Organometallics 15 (1996) 2790.

[24] M. Aizenberg, D. Milstein, J. Am. Chem. Soc. 117 (1995) 6456.

[25] F.A. Cotton, G. Wilkinson, Advanced Inorganic Chemistry, Wiley, New York, 1988, p. 777.

[26] M. Okazaki, H. Tobita, H. Ogino, The 42nd Symposium on Organometallic Chemistry, Hiroshima, Japan, Abstract PA221, 1995.

[27] M. Okazaki, H. Tobita, H. Ogino, J. Chem. Soc. Dalton Trans. (1997) 3531.

[28] S. Sakaki, M. Ieki, J. Am. Chem. Soc. 115 (1993) 2373.

[29] M. Loza, J.W. Faller, R.H. Crabtree, Inorg. Chem. 34 (1995) 2937.

[30] D.H. Berry, T.S. Koloski, P.J. Carroll, Organometallics 9 (1990) 2952.

[31] F. Ozawa, M. Kitaguchi, H. Katayama, Chem. Lett. (1999) 1289.

[32] (a) D.L. Thorn, J. Am. Chem. Soc. 102 (1980) 7109;
(b) D.L. Thorn, Organometallics 1 (1982) 197;
(c) R.T. Price, R.A. Andersen, E.L. Muetterties, J. Organomet. Chem. 376 (1989) 407.

[33] M. Aizenberg, D. Milstein, Organometallics 15 (1996) 3317.

[34] G.P. Mitchell, T.D. Tilley, Organometallics 14 (1995) 5472.

[35] M. Okazaki, H. Tobita, H. Ogino, Chem. Lett. (1997) 437.

[36] (a) K.H. Pannell, J. Cervantes, C. Hernandez, J. Cassias, S. Vincenti, Organometallics 5 (1986) 1056;
(b) H. Tobita, K. Ueno, H. Ogino, Chem. Lett. (1986) 1777;
(c) H. Tobita, K. Ueno, H. Ogino, Bull. Chem. Soc. Jpn. 61 (1988) 2797;
(d) K. Ueno, H. Tobita, H. Ogino, Chem. Lett. (1990) 369.

[37] (a) H. Tobita, K. Ueno, M. Shimoi, H. Ogino, J. Am. Chem. Soc. 112 (1990) 3415;
(b) T. Takeuchi, H. Tobita, H. Ogino, Organometallics 10 (1991) 835;
(c) H. Tobita, H. Wada, K. Ueno, H. Ogino, Organometallics 13 (1994) 2545;
(d) K. Ueno, A. Masuko, H. Ogino, Organometallics 18 (1999) 2694.

[38] M. Okazaki, Y. Kawano, H. Tobita, S. Inomata, H. Ogino, Chem. Lett. (1995) 1005.

[39] M. Okazaki, Y. Kawano, H. Tobita, S. Inomata, H. Ogino, J. Organomet. Chem. 553 (1998) 1.

[40] (a) H. Nakatsuji, J. Ushio, T. Yonezawa, J. Organomet. Chem. 258 (1983) C1;
(b) H. Jacobsen, T. Ziegler, Inorg. Chem. 35 (1996) 775;
(c) K. Ueno, H. Tobita, S. Seki, H. Ogino, Chem. Lett. (1993) 1723.

[41] R.D. Holmes-Smith, S.R. Stobart, R. Vefghi, M. Zaworotko, J. Chem. Soc. Dalton Trans. (1987) 969.

[42] U. Schubert, K. Bahr, J. Müller, J. Organomet. Chem. 327 (1987) 357.

[43] U. Schubert, H. Gilges, Organometallics 15 (1996) 2373.

[44] M.J. Auburn, R.D. Holmes-Smith, S.R. Stobart, M.J. Zworotko, T.S. Cameron, A. Kumari, J. Chem. Soc. Chem. Commun. (1983) 1523.

[45] (a) P. Hofmann, H. Heiss, P. Neiteler, G. Müller, J. Lachmann, Angew. Chem. Int. Ed. Engl. 29 (1990) 880;
(b) M. Hackett, J.A. Ibers, G.M. Whitesides, J. Am. Chem. Soc. 110 (1988) 1436;
(c) M. Hackett, G.M. Whitesides, J. Am. Chem. Soc. 110 (1988) 1449;
(d) P. Hofmann, H. Heiss, G. Müller, Z. Naturforsch. B 42 (1987) 395.